

# Towards Haptics-Enabled Robotic Surgery System

Yo-An Lim, Hyundo Choi and Junhyung Kim

**Abstract**—Stable and transparent haptic feedback in a teleoperated robotic surgery is still a challenging problem. In efforts to solve the problem, this paper presents a bilateral teleoperation system that is intended for minimally invasive robotic surgeries. The system consists of robot arms, haptic interfaces, linkage-driven surgical instruments, fiber Bragg grating (FBG)-based force sensors, a stereo endoscope, and a teleoperation controller. A novel force sensor that can measure 3-DoF force is designed, fabricated, and calibrated. Also, a novel linkage-driven surgical instrument with embedded ultrasonic actuators is designed and fabricated. Control algorithms for stable bilateral teleoperation is implemented for the system, and experiments on the silicone rubber are performed and preliminary results are shown.

## I. INTRODUCTION

Minimally invasive robotic surgery (MIRS) has been gaining much attention for the advantages in terms of patient outcomes compared to conventional minimally invasive surgery (MIS). The advantages of MIRS mostly come from better dexterity, precision, and depth perception at the surgical site due to teleoperated robots and high resolution stereo endoscopes. Although, teleoperation of robots enables surgeons to perform safer and more comfortable operations, it also has a challenging problem, that is, the lack of touch sensation during surgery.

Benefits of haptic feedback in MIRS have been reported in many research such as [1], [2], and thus it is thought that the necessity of haptic feedback is obvious. However, haptic feedback, especially force feedback is not clinically used in most robotic surgery systems, since it can potentially make the teleoperation system unstable and sensing the interacting force between the instrument and tissue is difficult. Many efforts to solve the stability problem of the teleoperation system have been made, and it is thought that stability control algorithms that were originally developed for haptic interactions in virtual reality environments such as [3], [4] are still promising in robotic surgery systems.

To give touch sensation to a user, force interacting between a surgical instrument and body tissue should be accurately measured. In that regard, research efforts for force sensing in MIRS have been made as in [5], [6]. For accurate force sensing, a force sensor should be attached near the surgical instrument tip that makes contact with body tissue, which requires a miniaturized force sensor. In addition, since the surgical instrument often accompanies a cautery that uses

high voltages, the force sensor should be immune to electromagnetic interferences (EMI), which means that a force sensor based on the electric strain gauge is not adequate for the purpose. Instead, optical fiber based, especially FBG-based, force sensors have been proposed for force sensing such as [7]. However, much attention should be paid when attaching optical fibers to sensing plates and managing fibers in the instruments.

Mostly in MIRS, actuators to operate surgical instruments are installed on a robotic arm, and they transmit complicated motions and proper force by use of cables. The cable-driven mechanisms have advantages such as easy bending, but they increase system backlash when their length increases. Moreover, long-term operation under high tension can permanently extend the cable length, which degrades the performance of the surgical instrument and increases the possibility of breakage. As another approach, linkage-driven mechanisms have been proposed as in [8], and they can exert tensile and compressive force while a cable can not apply compressive force, and a linkage can resist much higher tensile force.

In this paper, we present a bilateral teleoperation system for MIRS. A novel force sensor based on FBG is designed, fabricated, and calibrated. Also, the sensor is attached at the distal end of the novel linkage-driven surgical instrument with embedded ultrasonic actuators. In addition, the control architecture for the teleoperation system is discussed and a passivity-based algorithm is implemented for stable teleoperation. Surface following experiments on the silicone rubber are performed and the preliminary experiment results are shown.

## II. SYSTEM CONFIGURATION

In a functional viewpoint, the system connection can be summarized as in Fig. 2. A PC runs as a system controller

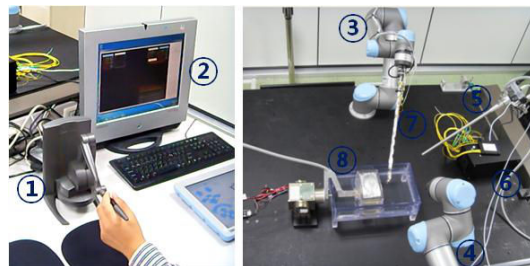


Fig. 1. System configuration (① haptic interface, ② control GUI, ③ slave robot 1, ④ slave robot 2, ⑤ stereo endoscope, ⑥ FBG interrogator, ⑦ surgical instrument, ⑧ silicone phantom)

The authors are with the Samsung Advanced Institute of Technology, Samsung Electronics, San 14, Nongseo-dong, Giheung-gu, Yongin-si, Gyeonggi-do, Korea. (e-mail: yoan.lim@samsung.com; hyundo.choi@samsung.com; riak.kim@samsung.com)

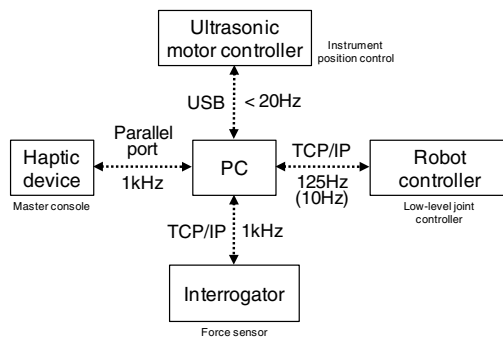


Fig. 2. System connection diagram

that integrates haptic interfaces, robot controller, ultrasonic motor controllers, and optical fiber interrogator.

### A. Force Sensor

A novel force sensor for MIRS is developed. The sensor is based on FBG-type strain gages and can measure 3-DoF force. A new flexible ring-shaped structure is designed and optimized using the finite element analysis to achieve the sensing range from -10 N to 10 N and sensitivity of 0.1 N with a diameter of 15 mm. Also, a stopper mechanism is added in the structure to avoid plastic deformation under unexpected large force.

1) *Design and Fabrication:* The sensor body design and the stress simulation result are shown in Fig. 3. The upper and lower bodies are connected through four horizontal beams and bolt holes, and square-shape regions for optical fiber holders are in the upper and lower end. Also, instead of being directly glued on the surface of the body, optical fibers are fixed to fiber holders that will be fixed on the sensor body. For the optimization of the sensor body structure, two design parameters, sensor body thickness and horizontal beam thickness, are selected and optimized using a finite element analysis.

2) *Calibration:* For the calibration of the FBG-based force sensor, a calibration jig including an octal-shaped component and a pulley for Z-axis loading, F-class weights, an interrogator (sm130, Micron Optics Inc.), and a data-processing PC are used as shown in Fig. 4. The octal-shaped component enables lateral loadings in 8 directions (45° intervals) and axial loadings in two directions ( $\pm Z$  directions), and the pulley is used to minimize the frictional

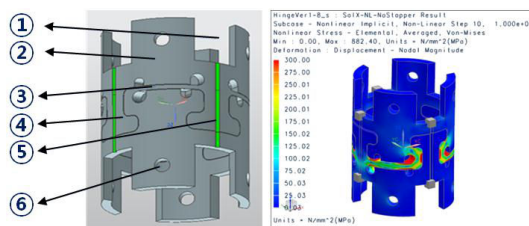


Fig. 3. Force sensor design and simulation (① fiber holder, ② sensor body, ③ horizontal beam, ④ stopper, ⑤ optical fiber sensor, ⑥ connecting bolt hole)

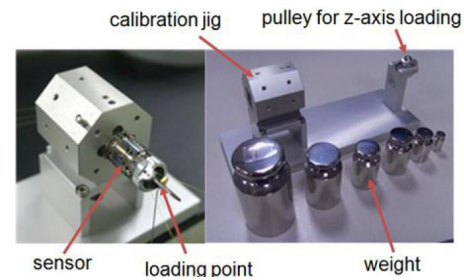


Fig. 4. Sensor calibration hardware

force during the Z-axis loading. In this work, loadings are applied in four lateral directions (0°, 90°, 180°, and 270° rotation) and  $\pm Z$  directions, and the calibration range and resolution for three axes are set to  $\pm 1200$  grams and 200 grams, respectively. Nonlinear characteristics that are mainly caused by inappropriate preloading and the associated misalignment of the attached fibers can be observed. Thus, a nonlinear approximation using an artificial neural network (ANN) is used for the calibration.

### B. Surgical Instrument

A linkage-driven surgical instrument with linear ultrasonic motors inside an elongated housing (dia. 15 mm) is designed and fabricated as in Fig. 5. The instrument can be divided into a driving rod module and a wrist module. In the driving rod module several ultrasonic motors are connected to two driving rods through flexible leaf springs that enable synchronized motion of a driving rod by compensating for the mechanical clearance and variations in the characteristics of ultrasonic motors. The wrist module is composed of two rotational joints, serially connected sliders, and intermediate linkages, and through linearly moving the driving rods, the joints can be rotated from +60° to -60° in the pitch and yaw directions.

1) *Driving Rod Module:* The developed surgical instrument is based on the embedded actuation method, which enables to obtain a compact surgical robot system and to easily append multiple wrist modules on a single instrument. Also, for the embedded actuation, miniaturized ultrasonic motors (Squiggle Micro Motor, New Scale Technology Inc.)

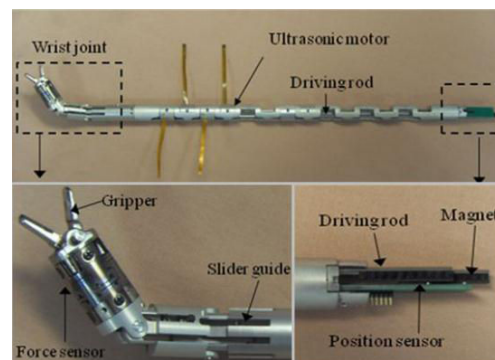


Fig. 5. Linkage-driven surgical instrument with embedded actuators

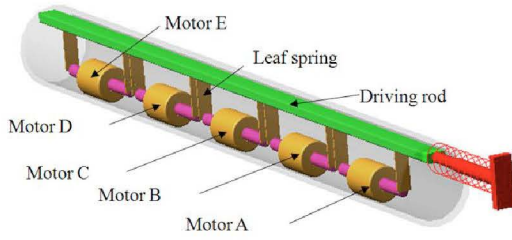


Fig. 6. Synchronization of ultrasonic motors using leaf springs

are used, since they have high power efficiency, millimeter-order size, and no reduction gears. However, the force generated by a motor is too small to drive a wrist joint. To solve this, several motors are connected to a driving rod through leaf springs as illustrated in Fig. 6, which produces enough rod force ( $> 10$  N) to drive the wrist mechanism. Through repeated experiments, it is confirmed that the driving rod can move with linear velocities of approximately 4.5 mm/s and 7.6 mm/s under a load of 10 N when five and six motors are connected, respectively. Also, when five motors are connected, the stall force of the rod is approximately 24 N.

2) *Wrist Module*: In the developed 2-DoF wrist mechanism, a slider-crank mechanism rotates the yaw frame, while the intermediate linkage guided by serially connected sliders moves the pitch frame. The yaw frame angle depends only on the displacement of the yaw driving rod. In contrast, the pitch frame depends on both the pitch driving rod and the yaw driving rod, because the linkage chain for the pitch motion is pivoted to the yaw frame with one of its linkages guided by the slider in the pitch frame.

### C. Master Device and Slave Robot

Two haptic interfaces (PHANToM Desktop, Sensable Inc.) and two industrial robots (UR5, Universal Robot) are used for master devices and slave robots, respectively. Assuming that the instrument is rigidly attached to the robot, the position and orientation of the master device are mapped to the position and orientation of the wrist, respectively. Also, a button of the master device is used for the on/off control of the instrument gripper position.

## III. SYSTEM CONTROL

The control structure of the teleoperated system is shown in Fig. 7. Basically, the overall system is a bilateral scaled teleoperation that includes force feedback and position/force scaling factors.

### A. Bilateral Teleoperation

As indicated in Fig. 7, when a user moves the master device, the position controller moves the robot to follow the scaled position of the master device. Also, when the robot makes contact with an environment, such as body tissues, the force sensor measures the contact force and the measured force is scaled and displayed to the master device, which usually resists the hand motion.

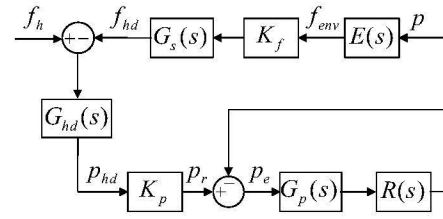


Fig. 7. Teleoperation control structure

In a bilateral teleoperation system, especially in a surgical system, stability is critical since unstable operations can be harmful to a patient, a user, and the system itself. Therefore, an algorithm that can guarantee stability must be included in the control system. In this work, the energy-bounding algorithm (EBA) [4] that was originally proposed as a stability algorithm for haptic interactions in virtual environments is implemented. The EBA is based on the passivity theorem and can ensure stable haptic interactions by limiting the energy generated by a sample-and-hold operator to stay within the energy that can be exhausted by the inherent damping elements in a haptic interface and by making the environment passive.

### B. Remote Center-of-Motion

Robotic systems for laparoscopic surgery mostly have the remote center-of-motion (RCM) mechanism that can maintain a position along the surgical instrument stationary. In this work, the system has a software RCM mechanism that can be realized by controlling the position and orientation of the robot, and an algorithm for the software RCM can be derived as depicted in Fig. 8. When the destination of the wrist is  $p_w = (x_w, y_w, z_w)$  and the trocar is located at  $p_t = (x_t, y_t, z_t)$ , the position where the robot should be moved becomes,

$$p_r = p_w - l \cdot r_p \quad (1)$$

where,  $l$  is the length of the instrument and  $r_p$  is the unit vector of the instrument orientation ( $\vec{p}_w - \vec{p}_t$ ), and the robot orientation should be the same as the instrument orientation.

### C. Coordinate Transformation

In MIRS, when moving the master device in a direction, the instrument displayed on a surgeon's screen should move

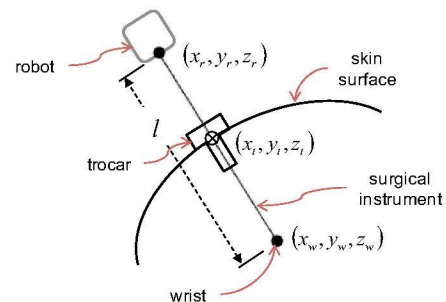


Fig. 8. Remote center-of-motion of surgical instrument

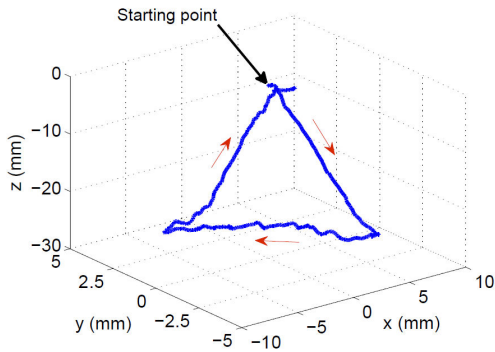


Fig. 9. End-effector trajectory

in the same direction. Therefore, the relationships between the coordinate systems of the master device, the robot, and the endoscope should be considered. Matching the directions can be accomplished by transforming the coordinate of the master device in the master device coordinate frame to the coordinated in the endoscope coordinate frame, which can be expressed as,

$$p_{hd}^{en} = R_r^{en} \cdot R_{hd}^r \cdot p_{hd} \quad (2)$$

where,  $p_{hd}^{en}$  and  $p_{hd}$  are the positions of the master device in the endoscope and the master device coordinate frame, respectively. Also,  $R_r^{en}$  and  $R_{hd}^r$  are the rotational matrices that relates the endoscope–robot frames and the robot–master device frames, respectively.

#### IV. EXPERIMENTS

Experiments, such as contacting and following the surface of the silicone rubber, were performed. A spatula-shaped end-effector was attached at one end of the force sensor instead of a gripper. During experiments, a user teleoperated the end-effector and when the end-effector made contact with the rubber the force sensor measured the interacting force and the force was scaled up and then displayed to the master device. In this work, the position and force scaling factors were set to 1 and 10, respectively. Note that the force sensor also measures the inertial force when in non-contact motion, thus a user can feel some resisting force even in free motion, which induces transparency problems in a bilateral teleoperation system. Transparency in free motion as well as in contact should be a research issue for more immersive bilateral teleoperation.

In surface following experiments, users were asked to make the end-effector follow the surface of the rubber without applying excessive force, and Figs. 9 and 10 show the trajectory of the end-effector and the measured force of an experiment, respectively. In the results, abrupt changes in the measured force can be observed, which is caused by the sticky and rough surface of the rubber. Also, the measured force is relatively small and within a bound, which means no excessive force applied to the rubber during following. Through experiments, it is confirmed that the force feedback

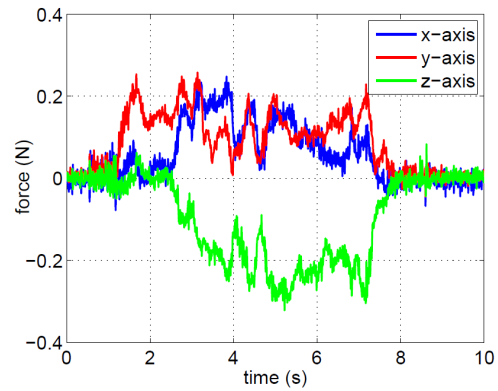


Fig. 10. Measured force

is very helpful to identify the contact instant and keep the contact force within a bound.

#### V. CONCLUSIONS AND FURTHER WORK

In an effort for haptic feedback in MIRS, a bilateral teleoperation system is developed. A novel FBG-based 3-DoF force sensor and a linkage-driven surgical instruments are designed and fabricated. Also, a passivity-based algorithm is implemented for the stability of the scaled bilateral teleoperation. Preliminary experiment results show that with the developed bilateral control system a user can follow the surface of the rubber with small and bounded contact force. Also, the perception of a contact instant is faster and easier with the haptic feedback than only with the stereo visual display.

#### REFERENCES

- [1] C. R. Wagner, N. Stylopoulos, P. G. Jackson, and R. D. Howe, "The benefit of force feedback in surgery: Examination of blunt dissection," *Presence: Teleoperators and Virtual Environments*, vol. 16, no. 3, pp. 252–262, 2007.
- [2] A. M. Okamura, "Haptic feedback in robot-assisted minimally invasive surgery," *Current Opinion in Urology*, vol. 19, no. 1, pp. 102–107, 2009.
- [3] B. Hannaford and J.-H. Ryu, "Time-domain passivity control of haptic interfaces," *IEEE Transactions on Robotics and Automation*, vol. 18, pp. 1–10, 2002.
- [4] J.-P. Kim and J. Ryu, "Robustly stable haptic interaction control using an energy-bounding algorithm," *International Journal of Robotic Research*, vol. 29, no. 6, pp. 666–679, 2010.
- [5] N. Zemiti, G. Morel, T. Ortmaier, and N. Bonnet, "Mechatronic design of a new robot for force control in minimally invasive surgery," *IEEE/ASME Transactions on Mechatronics*, vol. 12, no. 2, pp. 143–153, 2007.
- [6] G. Tholey and J. P. Desai, "A modular, automated laparoscopic grasper with three-dimensional force measurement capability," in *Proceedings of the 2007 IEEE International Conference on Robotics and Automation*, Roma, Italy, April 2007, pp. 250–255.
- [7] Y.-L. Park, S. C. Ryu, R. J. Black, B. Moslehi, , and M. R. Cutkosky, "Fingertip force control with embedded fiber bragg grating sensors," in *2008 IEEE International Conference on Robotics and Automation*, Pasadena, USA, May 2008, pp. 3431–3436.
- [8] Y. Sekiguchi, Y. Kobayashi, Y. Tomono, H. Watanabe, K. Toyoda, K. Konishi, M. Tomikawa, S. Ieiri, K. Tanoue, M. Hashizume, and M. G. Fujie, "Development of a tool manipulator driven by a flexible shaft for single port endoscopic surgery," in *Proceedings of the 2010 3rd IEEE RAS & EMBS International Conference on Biomedical Robotics and Biomechatronics*, Tokyo, Japan, September 2010, pp. 120–125.